*Glm*S mediated knock-down of a phospholipase expedite alternate pathway to generate phosphocholine required for phosphatidylcholine synthesis in *Plasmodium falciparum*

Pradeep Kumar Sheokand, Monika Narwal, Vandana Thakur and Asif Mohmmed*

International Centre for Genetic Engineering and Biotechnology, New Delhi 110 067, India.

* Corresponding Author

Tel.: +91 11 2674 1358; FAX: +91 11 2674 2316

E-mail address: amohd@icgeb.res.in

Abstract

Phospholipid synthesis is crucial for membrane proliferation in malaria parasites during the entire cycle in the host cell. The major phospholipid of parasite membranes, phosphatidylcholine (PC), is mainly synthesized through the Kennedy pathway. The phosphocholine required for this synthetic pathway is generated by phosphorylation of choline derived from catabolism of the lyso-phosphatidylcholine (LPC) scavenged from the host milieu. Here we have characterized a *Plasmodium falciparum* lysophospholipase (*Pf*LPL20) which showed enzymatic activity on LPC substrate to generate choline. Using GFP- targeting approach, *Pf*LPL20 was localized in vesicular structures associated with the neutral lipid storage bodies present juxtaposed to the food-vacuole. The C-terminal tagged *glmS* mediated inducible knock-down of *Pf*LPL20 caused transient hindrance in the parasite development, however, the parasites were able to multiply efficiently, suggesting that *Pf*LPL20 is not essential for the parasite. However, in *Pf*LPL20 depleted parasites, transcript levels of enzyme of SDPM pathway (Serine Decarboxylase-Phosphoethanolamine Methyltransferase) were altered along with upregulation of phosphocholine and SAM levels; these results show upregulation of alternate pathway to generate the phosphocholine required for PC synthesis through the Kennedy pathway. Our study highlights presence of alternate pathways for lipid homeostasis/membrane-biogenesis in the parasite; these data could be useful to design future therapeutic approaches targeting phospholipid metabolism in the parasite.

Keywords: Malaria, *Plasmodium falciparum*, phospholipase, phospholipid-synthesis, lipid-homeostasis

Introduction

Malaria is a major vector-borne infectious disease caused by a protozoan parasite, *Plasmodium spp.*, which is particularly rampant in tropical and subtropical regions of the world. Globally there are more than 229 million cases of malaria worldwide in 2019, and the majority of those, approximately 213 million, were from the African region. This parasitic disease cause ~400,000 deaths globally and the most vulnerable group are the children aged under 5 years [1, 2]. In absence of an efficient vaccine for malaria as well as due to the rise of drug-resistant parasite strains, there is an urgent need to identify new drug-targets and development of effective antimalarial. Understanding of key metabolic pathways in the parasite which are essential for parasite survival remains to be the pre-requisite to identify unique and potent targets in the parasites.

The malaria parasite has a complex life cycle in the mosquito vector and human host, having multiple developmental stages. The pathological symptoms are caused by the repeated asexual blood-stage cycle. During the asexual cycle, the parasite replicates rapidly inside the host erythrocyte which requires a vast amount of lipids to support extensive membrane biogenesis for its growth and segregation [3]. These demands can be fulfilled by scavenging the host cell lipid and use them after degradation/modification as well as through *de novo* synthesis of fatty acids and phospholipids [4-7]. Phospholipids, including phosphatidylcholine (PC), phosphatidylethanolamine (PE), and phosphatidylserine (PS), are the major structural components of the parasite membranes, which have a little amount of cholesterol [8]. In the uninfected erythrocytes, the share of these phospholipids, PC, PE, PS, is 30-40%, 25-35%, and 10-20%, respectively; however, parasites/infected erythrocytes contain 20-55% of PC, 15-40% of PE and 4-15% PS [9, 10].

The phosphatidylcholine is a major membrane phospholipid, which can be synthesized in *Plasmodium* parasites by two routes including the cytidine diphosphate- or CDP-choline

branch of the Kennedy pathway and the Serine Decarboxylase-Phosphoethanolamine Methyltransferase (SDPM) pathway. The Kennedy pathway is responsible for 89% of PC synthesis in the parasite using choline; the choline first gets converted into phosphocholine by the action of choline kinase and then enters in the Kennedy pathway [11]. The SDPM pathway involves five enzymes that uses host serine and fatty acids as precursors for PC synthesis. There are three sequential methylation steps of phosphoethanolamine by phosphoethanolamine methyltransferase (*Pf*PMT) produce phosphocholine, which then enters in the Kennedy pathway [12-14]. It has been shown that PC synthesis uses choline generated from the catabolism of lysophosphatidylcholine scavenged in the host milieu [9]. A recent study suggested that lysophosphatidylcholine (LPC) is essential to maintain the asexual cycle, whereas in LPC depleted conditions the parasites switch to the sexual commitment [15]. To obtain the phospholipid building blocks, complex phospholipids obtained from the host are to be catabolized by the action of hydrolases including phospholipases and lysophospholipases [16-18]. Phospholipases are classified into four groups (A, B, C, D) depending on their lipolytic activity. Phospholipase A (PLA) and B (PLB) break the acyl ester bond whereas Phospholipase C (PLC) and D (PLD) target the phosphodiesterase bonds. Therefore, phospholipases are responsible for generation of fatty acids (FAs) and lysophospholipids (LPC, LPE, LPS). Lysophospholipases (LPLs) are also classified on the basis of their cleavage sites. The *P. falciparum* genome codes for 14 putative LPLs, out of which ten LPLs have high sequence similarity (36-61%) with each other; these proteins are ~400 amino acid long without having any signal sequences [19]. The other four LPLs are 675-921 amino acid long and have a signal peptide. The characteristic GXSXG motif is conserved among all lysophospholipases wherein, the active site residue serine (S) is flanked by the glycine. The catalytic triad is composed of serine (S), aspartate (D), and histidine (H). Several studies have characterized parasite phospholipases

in the malaria parasite for their role in asexual and gametocytic stages of the parasites [20, 21]. One of the most characterized α/β hydrolases is an esterase, *Pf*PARE (*PF*3D7_0709700), although this gene is not essential at the asexual blood stage of the parasite, but its expression changes in pepstatin-resistant parasites [22]. Another *Plasmodium* protein with phospholipase activity was found to play role in hepatocytic egression [23]. Conditional knock-down of *Pf*PAPTPL1 (Patatin like phospholipase 1) showed that it is dispensable for the asexual staged but *Pf*PAPTPL1 depleted gametocytes have reduced flagellation and egress. In contrast to this, delayed gametocyte maturation has been observed in PNPLA1/PATPL depleted parasites instead of the defect in flagellation [20, 21]. LPLs are also expected to play role in the catabolism of host-derived complex lipids, such as LPC, to obtain building blocks for parasite phospholipid synthesis. However, there are very few studies for the localization and functional significance of parasite lysophospholipases.

Here, we report the biochemical and functional characterization of one of the *P. falciparum* LPL, named *Pf*LPL20 (PlasmoDB gene ID: PF3D7_0702200). The recombinant *Pf*LPL20 was expressed, purified and its LPL specific enzymatic activity was confirmed. We used the GFP-*glmS* ribozyme system for localization and conditional knockdown of the native protein in the parasite. The protein was found to be associated with the neutral lipid storing bodies in the asexual blood-stage parasites; efficient growth of parasites under conditional knockdown of *Pf*LPL20 confirms its dispensability for parasite survival. However, alteration in the SDPM pathway genes expression and accumulation of phosphocholine as well as S-adenosylmethionine in the *Pf*LPL20 depleted parasites, indicated a switch to the SDPM pathway to generate the phosphocholine required for the Kennedy pathway-dependent synthesis of PC.

Material and methods

Parasite culture, plasmid construct, and parasite transfection

Plasmodium falciparum strain 3D7 was cultured in RPMI media (Invitrogen) supplemented with 0.5% (w/v) Albumax (Invitrogen) 4% haematocrit. The culture was kept static in a gas mixture of 5% carbon dioxide, 5% oxygen, and 90% nitrogen at 37°C. To generate an overexpression line, the full-length *pfLPL20* gene was amplified using primers 1294A, 1295A and cloned into pSSPF2-GFP vector. Parasite cultures were synchronized by repeated sorbitol treatment and 100 μg of purified plasmid DNA (Plasmid Midi Kit, Qiagen, Valencia, CA) was transfected in *P. falciparum* by electroporation (310 V, 950 μF) [43]. Transfected parasites were selected over 2.5 μg/ml blasticidin (Calbiochem). To generate *Pf*LPL20-glmS-GFP construct, C-terminal fragment (750 bp long) of *pfLPL20* gene was amplified using specific primers 1224A and 1225A and cloned into *glm*S-GFP vector [44]. The C-terminal fragment was cloned in-frame to the N-terminus of GFP in the *Spe*I and *Kpn*I restriction enzymes sites. Transfected parasites were selected over 2.5 μg/ml blasticidin (Calbiochem) and subsequently subjected to on and off cycling of blasticidin drug to promote the integration of the plasmid in the main genome. Integration was confirmed by PCR using 2200F and 1234A and by western blotting also by using an anti-GFP antibody. Individual parasite clones were isolated by serial dilution method, and integration was confirmed in the clonal parasite population.

Conditional knock-down analysis and in-vitro growth assays

To assess the effect of knock-down of *Pf*LPL20 on the parasite, *Pf*LPL20-*glmS*-GFP transgenic parasites were tightly synchronized with 5% sorbitol and grown with media containing 2.5mM concentration of glucosamine (GlcN) (Sigma-Aldrich) or solvent alone (incomplete media, iRPMI). For microscopic analysis and morphology of the parasites,

Giemsa-stained smears were prepared at every 8hr interval from both glucosamine treated and control parasites. Parasite growth was assessed after 48 and 96 hours by flow cytometry using BD FACS Calibur (Beckton Dickinson). Briefly, cells were incubated with EtBr for 30 minutes at 37°C in dark followed by two washing with 1×PBS. These samples were analyzed by fluorescence counting, 100,000 events were acquired using BD FACS Calibur system (Beckton Dickinson); EtBr-stained uninfected erythrocytes were used as background control. To assess the effect of glucosamine on the down regulation of *Pf*LPL20 at the protein level, *Pf*LPL20-GFP-glmS ring stage parasites were treated with 2.5 mM glucosamine, harvested at the schizont stage, and subjected to the western blotting.

Parasite fractionation and Western blotting

Parasites were harvested at the trophozoite stage by lysis of infected RBCs using 0.15% saponin; the supernatant was collected separately, and the parasites pellet was lysed by the freeze-thaw cycle. Laemmli buffer was added to both the fractions and proteins were separated in 12% SDS-PAGE. Subsequently, fractionated proteins were transferred to PVDF membrane (Millipore) and incubated with blocking buffer (4% skim milk or 3% BSA in 1× PBS). Blots were incubated with primary antibody (rabbit anti-GFP 1:10000, rabbit anti-BiP 1:15000), washed 5 times with 1×PBS, and probed with HRP conjugated respective secondary antibody (1:100000). Subsequently, blots were washed with 1×PBS and visualized using a thermo-scientific ECL kit.

Immuno-fluorescence assay (IFA) and fluorescent microscopy

Infected RBCs were fixed in 4% paraformaldehyde and 0.05 % glutaraldehyde. After permeabilization with 0.1 % TritonX-100, the cells were incubated with rabbit polyclonal anti-GFP (1:500) for 2 hours and subsequently labelled with Alexa Flour-488. Labeled

parasites were washed three times with 1×PBS. Parasite nuclei were stained with DAPI at a final concentration of 5 µg/ml. To label the neutral lipid storage structures, parasites were stained with Nile Red (Molecular Probes) using a modified method [34]. Briefly, Nile Red was added to a final concentration of 1 µg/ml into the parasite culture (5-10% parasitemia), the culture was incubated on ice for 30 min and subsequently washed with 1×PBS before analysis by confocal microscopy. Images were captured by Nikon A1 confocal laser scanning microscope and analysed by Nikon-NIS element software (version 4.1). The 3D images were constructed by using series of Z-stack images using IMARIS 7.0 (Bitplane Scientific) software.

Quantitative real-time PCR

For transcriptional analysis of different genes, RNA was extracted using the TRIzol method from both control and glucosamine treated parasite culture; reverse transcribed using the iScript cDNA Synthesis Kit (Bio-Rad) following manufacturer's recommendations. Real-time amplification reactions were performed in triplicate on the StepOnePlus™ Real-Time PCR System (Applied Biosystems, Foster City, CA, USA) using a SYBR Green master-mix from Biorad (CA, USA). Each reaction comprised an equal amount of cDNA, 100 ng of both the gene-specific primers for the target gene [*pfLPL20*, *pfPMT* (phosphoethanolamine-methyltransferase), *pfSAMS* (S-adenosylmethioninesynthetase), *pfEK* (ethanolamine kinase), and *pfCK* (choline kinase) (see supplementary Table S1)], and 1× SYBR Green PCR mix. The threshold cycles (CTs) generated by qPCR system were used to calculate fold change for relative quantitative analysis. Each assay was carried out in triplicate, and the experiments were repeated thrice.

LC-MS analysis for estimation of choline, phosphocholine, and S-adenosylmethionine

Parasites were isolated from Infected red blood cells (5×10^7 cell equivalents) from both *Pf*LPL20-iKD and control by using saponin lysis. Their total lipids were extracted by chloroform: methanol, 1:2 (v/v) and chloroform: methanol, 2:1 (v/v) as previously described [4]. The standard compounds (choline, phosphocholine, and S-adenosylmethionine) were purchased from Sigma-Aldrich in form of choline chloride, phosphorylcholine chloride calcium salt tetrahydrate, and S-(5′-Adenosyl)-L-methionine p-toluene sulfonate salt and were dissolved in HPLC grade solvents. Samples were analyzed by 3200-QTRAP LC-MS system for estimation as described previously [45].

Expression, and purification of recombinant protein

Full-length *pfLPL20* gene was amplified by using specific primers 2200F and 2200R and cloned into pETM41 vector between *Nco*I and *Xho*I sites to give pETM41-His6-MBP-*Pf*LPL20 construct. The recombinant protein *PfLPL20* was expressed as a soluble protein in the cytosol of the *E. coli* BL21(DE3) codon$^+$ cells. For expression, bacterial cells having pETM41-His6-MBP-*Pf*LPL20 were grown in LB medium supplemented with kanamycin at 37°C. Expression of the fusion protein was induced using 1mM isopropyl β-D-thiogalactoside (IPTG) overnight at 16°C. The next day, cells were harvested and resuspended into lysis buffer (25mM Tris, pH7.4, 500mM NaCl, 10mM Imidazole) and lysed by sonication (Vibra cell sonicator). The supernatant was subjected to a combination of Ni-NTA affinity chromatography followed by amylose affinity chromatography. Eluted fractions were subjected to SDS-PAGE to assess the purity of the recombinant protein.

Lysophospholipase (LPL) activity assay using LPC as substrate and enzyme kinetics

For assessing the enzymatic activity of the recombinant *Pf*LPL20, a lysophospholipase (LPL) activity assay was established using lysophosphatidylcholine as substrate. The activity

assay reaction mixture (200µl total volume) contained 16:0 lysophosphatidylcholine (LPC) as substrate, 20µg (285 pmol) of recombinant protein, 0.1 unit glycerophosphodiestrase (Sigma), 0.2 U/ml choline oxidase (Sigma 26978), 2U/ml horseradish peroxidase (Sigma P8125), 100µM Amplex Red (Invitrogen) in a reaction buffer (50mM Tris pH 8.0, 5mM $CaCl_2$). In this assay, the LPL cleaves the acyl chain from LPC resulting in the generation of glycerophosphocholine on which glycerophosphodiestrase acts and release the choline moiety. This choline was oxidized by choline oxidase to produce betaine and H_2O_2. Finally, H_2O_2 in presence of horseradish peroxidase reacts with Amplex Red reagent in 1:1 stoichiometry to generate the highly fluorescent product resorufin. The LPL activity was monitored by measuring fluorescence intensities (530/590 nm) for 6 hrs using Spectramax M2 microplate reader. The assay was performed by varying the amount of protein and substrate to get optimum LPL activity. For calculating the kinetic parameter, *K*m, the varied concentration of the LPC substrate (0-100 µM) at constant enzyme concentration (20µg) was set up in a reaction plate in triplicate. The kinetic constant *K*m was determined by fitting the Michalies-Menten curve using the Graph Pad Prism V5.0 software with 95 % confidence intervals.

Statistical Analysis

The data sets were analysed using GraphPad Prism ver 5.0 to calculate *K*m value and the datasets were compared using unpaired Student's *t*-test.

Results:

PfLPL20 is an active lysophospholipase having an alpha/beta hydrolase domain

*Pf*LPL20 is 424 amino acid long 49.9 kDa protein having putative transmembrane region (37 to 55 amino acids) and two hydrolase domains (82- 151 aa and 194 -386 aa; Pfam PF12146 E-value $2.3e^{-05}$ and $2.2e^{-14}$ respectively) (Figure 1A). Although both the domains contain characteristic hydrolase motif GXSXG, the three active site residues (S218, D349, H375) are present only in the second hydrolase domain (Supplementary figure 1). The active site S218 residue in the conserved motif is located in the characteristic 'nucleophile elbow' of hydrolase domains [24]. *Pf*LPL20 is annotated as a putative lysophospholipase in the *Plasmodium* genome database, PlasmoDB. To ascertain and characterize the enzymatic activity of *Pf*LPL20, recombinant protein corresponding to full-length gene was expressed using *E. coli* expression system and purified by using a combination of affinity chromatography techniques. The purified recombinant-*Pf*LPL20 migrated as ~90kDa protein on SDS-PAGE, which is slightly above the expected size of ~84kDa (Figure 1B). The purified recombinant protein was used in a fluorescence-based activity assay of lysophospholipase using LPC substrate (Figure 1C). The recombinant *Pf*LPL20 showed concentration dependent activity in the assay, confirming it to be a lysophospholipase. The *K*m value enzyme was found to be 33.41µM and the R^2 value for the kinetics was found to be 0.955. (Figure 1D).

Stage specific subcellular localization of PfLPL20

To study the localization of *Pf*LPL20 in asexual stage parasites, we generated the transgenic parasite line for episomal expression of *Pf*LPL20-GFP fusion protein. Expression of the fusion protein was confirmed by western blotting (Figure 2A), and these transgenic parasites were studied for localization of the *Pf*LPL20-GFP fusion protein by fluorescence/confocal

microscopy. The GFP signal was not observed in the ring stage parasites, but as the parasite developed through the trophozoite and schizont stage, the fluorescence signal was observed in vesicular structures in the parasite cytosol. During trophozoite stages, the *Pf*LPL20 was present in distinct foci/vesicle at the parasite periphery, close to the parasite membrane; in addition, some of these vesicles were also distributed in the cytosol (Figure 2B); in late-trophozoite and schizont stages, the fluorescence was observed in 2-3 large vesicular structure and several of these structures were present close to the food-vacuole (Figure 2B). Three-dimensional reconstruction of confocal images also shows the distribution of these vesicles in the cytosol (Supplementary Movie-1). The size and location of these large vesicular structures resemble the food-vacuole associated lipid-storage bodies in the parasites. We assessed localization of *Pf*LPL20 with respect to lipid storage vesicles by co-staining the transgenic parasites with Nile Red. The Nile Red is a hydrophobic probe that stains lipid storages in cells and concentrates in stores of neutral lipids such as TAG [7]. In trophozoite and schizont stage parasites, the Nile Red stained 1-2 vesicular structures closely associated with food vacuole (Figure 2C). The Nile Red stained lipid bodies showed complete overlap with *Pf*LPL20-GFP near the food vacuole, suggesting that the *Pf*LPL20 localize in the neutral lipid storage bodies (Figure 2C). Three-dimensional reconstruction of confocal images shows a clear overlap of GFP and Nile Red staining (Supplementary Movie-2). As these lipid bodies are membrane-bound structures, we also stained the parasite with lipid probe, BODIPY TR-ceramide; GFP labelled vesicles near the food-vacuole showed overlap with the BODIPY staining (Figure S2).

Endogenous tagging of pfLPL20 gene to generate PfLPL20-GFP-glmS transgenic parasite

We tagged the endogenous *Pf*LPL20 to study its functional essentiality by conditional knock-down strategy. We used GFP-*glm*S ribozyme system for C-terminal tagging of the native *pfLPL20* gene by single cross-over, so that the fusion protein gets expressed under the control of the native promoter (Figure 3A). A transgenic parasite line, *Pf*LPL20-GFP-*glm*S, was obtained and individual parasite clones were isolated; C-terminal integration was confirmed using PCR-based analyses (Figure 3B). Expression of the fusion protein of ~70kDa was detected by western blot analysis using anti-GFP antibody (Figure 3C); this band was not detected in wild type 3D7 parasites. Further, western blot analysis for different parasite developmental stages, showed expression at all the stages, with trophozoites having the maximum expression levels (Figure 3D). Localization of endogenously tagged *Pf*LPL20-GFP protein showed similar localization as in the case of episomally expressed protein. The GFP signal in these parasites was observed in vesicular structures in the parasite cytosol as distinct foci/vesicle during trophozoite stages, whereas during late-trophozoite and schizont stages, the labelling was observed in large vesicular structure present juxtaposed to the food-vacuole (Figure 3E). Further, staining with Nile red showed that these vesicular structures are neutral lipid-rich body; Nile red staining showed overlap with the endogenously tagged *Pf*LPL20-GFP protein in these structures (Figure 3F).

PfLPL20 is dispensable at the asexual stage of the parasite

To understand the functional significance of *Pf*LPL20 and its possible involvement in lipid metabolism, we utilized the transgenic *Pf*LPL20-GFP-*glmS* parasite line for *glmS* ribozyme mediated inducible knock-down of *Pf*LPL20 expression. Inducible knock-down (iKD) of *pfLPL20* was assessed by estimating corresponding mRNA levels as well as levels of *Pf*LPL20-GFP protein in the parasite cultures grown in presence of glucosamine (*Pf*LPL20-iKD set) as compared to the control set. The glucosamine treatment significantly reduced

the *Pf*LPL20-GFP levels in the *Pf*LPL20-iKD set (Figure 4A, B). To assess the effect of this *Pf*LPL20 knock-down on parasite growth, synchronized parasite cultures were grown in the presence or absence of glucosamine, and new ring-stage parasites were counted for two subsequent cell-cycles using flow-cytometry as well as using Giemsa stained smears of parasite cultures. However, we could not observe any change in the parasite growth in *Pf*LPL20-iKD set as compared to controls (Figure 4D), which may indicate the dispensability of this gene for the asexual blood-stage parasite.

Further, to study the effect of selective degradation of *Pf*LPL20 on the parasite development cycle, Giemsa-stained smears of the parasites were prepared at different time points during the assay. In the control set, during each intra-erythrocytic cycle, the parasites developed from ring to trophozoites to mature schizonts, and subsequently, merozoites released from these schizonts invaded new erythrocytes, which effectively increased the total parasitemia. In *Pf*LPL20-iKD set, the parasites developed from ring to trophozoites stages, however, several trophozoites showed an interruption in further development (Figure 4E). It was observed that this growth interruption was only transient, which led to a slight delay in parasite development, however, all the parasites were able to develop into mature stages and overall parasite growth and multiplication was similar as in the case of the control set. As described above, the *Pf*LPL20 was localized in a neutral lipid body present juxtaposed to the food-vacuole, therefore, we assessed the effect of *Pf*LPL20 knockdown on these lipid bodies. However, there was no change in the size or Nile Red staining of neutral lipid bodies in the *Pf*LPL20-iKD parasites (Figure S3).

PfLPL20 knock-down affect the homeostasis of phosphatidylcholine synthesis pathways

P. falciparum utilizes two pathways for bio-synthesis of phosphatidylcholine (PC): (i) CDP-Choline branch of the Kennedy pathway; and (ii) Serine Decarboxylase-

Phosphoethanolamine Methyltransferase (SDPM) Pathway. Depletion of LPC has been shown to influence phosphatidylcholine synthesis pathways in the parasite through induction of SDMP pathway genes and shift towards using Serine or Ethanolamine as preferential substrate. Since *Pf*LPL20 is involved in cleavage LPC, hence its knock-down may deplete the production of choline substrate required for PC synthesis and thus mimic LPC depleted conditions; therefore, we assessed if this influence the expression level of genes of PC-biosynthesis as suggested by Brancucci et al. Real-time quantitative PCR based analyses was carried out for genes *pfSAMS, pfPMT, pfEK* as well as for *pfLPL20*. In addition, we also assessed transcript levels of choline kinase, *pfCK*, which is also plays role in phosphocholine generation in the PC synthesis pathway. As described above, there was a significant reduction (>60%) of the *pfLPL20* in the *Pf*LPL20-iKD set as compared to the control set; whereas, *pfSAMS* expression level was significantly increased ~3.5 fold in the *Pf*LPL20-iKD set. There was no change in the expression levels of *pfPMT, pfEK, and pfCK* (Figure 5A).

The upregulation of *pfSAMS* in *Pf*LPL20-iKD conditions suggests that SDPM pathway may have switched higher synthesis of choline-phosphate, which could be utilized for PC-synthesis by the Kennedy pathway. We compared the levels of choline, phosphocholine, and SAM in *Pf*LPL20-iKD set as compared to the control set. The LC-MS analysis showed that there was no significant change in the choline levels for the two sets (Figure 5B), however, phosphocholine levels were significantly high in *Pf*LPL20-iKD set as compared to control (Figure 5C), in addition, SAM levels were also found to be upregulated in *Pf*LPL20-iKD set as compared to control (Figure 5D). This data correlated with the upregulation of SDPM pathway in the knock-down conditions.

Discussion

The asexual growth cycle of the malaria parasite involves an extensive synthesis of lipids, especially those required for the development of new membranes. Indeed, there is a huge increase in phospholipids, neutral lipids, and fatty acids content in the parasite as it develops inside the host erythrocyte [25]. Several studies showed that the metabolic pathways linked with synthesis, catabolism, and trafficking of lipids, are essential for parasite survival [17, 26-28]. The parasite can carry out *de novo* synthesis as well as scavenge lipids/phospholipids from the host milieu during the erythrocytic cycle, which are metabolized and used for its growth.

In our attempts to further understand lipid homeostasis and membrane synthesis in the parasite, we explored the role of a putative lysophospholipase (LPL) in *P. falciparum*. In *P. falciparum*-infected erythrocytes, lysophospholipase-like activity was found to be increased up to 3-fold [29], suggesting functional relevance of this enzyme for parasite growth and segregation. We have carried out the biochemical and functional characterization of putative a lysophospholipase, labelled as *Pf*LPL20 (Gene ID: PF3D7_0702200). The *P. falciparum* genome codes for a large family of about 14 LPLs, however, their functional roles are not characterized for many of the LPLs. All the LPLs harbors α/β hydrolase domain having GXSXG conserved motif. *Pf*LPL20 also contains this conserved motif having serine, histidine, and aspartic acid as catalytic site residues, conserved for all the lysophospholipases across kingdoms. The recombinant *Pf*LPL20 showed LPL specific activity utilizing LPC as substrate. Indeed, it is shown that the LPC scavenged from the host milieu is used to generate metabolites to be utilized by the parasite for its growth [9].

Enormous research has been carried out to develop different reverse genetic approaches for gene function analysis in malaria parasites [30]. As it is difficult to knock-out an essential gene in the parasite, several tools have been developed for transient knock-down of the target gene in the parasite [31, 32]. We used the *glm*S ribozyme system for

conditional knock-down of the target gene; we tagged *Pf*LPL20 at C-terminal with GFP-*glm*S tag, so that the transgenic parasites can be studied for both localization and gene function analysis. In addition, a transgenic parasite line expressing *Pf*LPL20-GFP fusion protein was also generated for localization studies. Confocal microscopic analysis of both transgenic parasite lines (*Pf*LPL20-GFP and *Pf*LPL20-GFP-*glm*S) showed that *Pf*LPL20 is present in vesicular structures, which are associated with parasite membrane or distributed in the parasite cytosol; in late stages, these vesicles fused in a large vesicular structure close to the food-vacuole. These structures showed resemblance with the previously reported neutral lipid bodies (NLB) [33, 34], which act as a reservoir of diacylglycerols (DAG) and triacylglycerol (TAG). Co-localization of *Pf*LPL20 with neutral lipid markers confirmed its presence in these lipid bodies. It is suggested that the parasite utilizes these stored lipids for membrane biogenesis during segregation. Localization of *Pf*LPL20 in small endocytic vesicles near parasitophorous vacuole and its subsequent localization in neutral lipid stores may indicate its involvement in the catabolism of lipids that are scavenged from the host. Indeed, it has been shown that *P. falciparum* scavenges LPC from the host milieu which gets catabolized and utilized in PC synthesis required for membrane biogenesis [9]. As expected from sequence homology and presence of the catalytic active site, *Pf*LPL20 showed catabolic activity on LPC substrate, which may suggest its role in phospholipid recycling in the parasite. Overall, the localization studies and biochemical characterization of *Pf*LPL20 indicate its association with lipid homeostasis in the parasite.

The C-terminal *glm*S tag-based system could induce >60% knock-down of *pfLPL20* transcript in the transgenic parasites; whereas the parasite growth analysis showed that the inducible-knock-down did not affect the parasite growth and multiplication, which may suggest that the enzyme is not essential for the survival of the asexual blood-stage parasites. A recent study using *piggyBac* transposon insertion-based mutagenesis study also showed

the dispensability of *Pf*LPL20 [35]. *Pf*LPL20 shows a high degree of similarity with another hydrolase (*Pf*PARE), which is also not essential at the asexual stage but mutations in this gene are responsible for resistance to new potential drugs [22]. One of the reasons for dispensability of an active enzyme in the cell could be compensation of its function by any other enzymes/pathway. Biochemical characterization shows that catabolism of LPC is the main function of *Pf*LPL20 which generates fatty acids and choline to be utilized by the parasite. Although the parasite can import free choline from the host milieu [36, 37], however, the scavenged choline is not utilized by the parasite for membrane synthesis [9]. Detailed analysis of parasite stage development in the *Pf*LPL20 knockdown suggested transient morphological effects on trophozoite stages. These results may suggest the possibility that the *Pf*LPL20 function is compensated or switched over to another metabolic pathway in the parasite. *P. falciparum* harbours more than ten LPLs, and it is possible that any other LPL takes over the function of *Pf*LPL20 under its knockout conditions. Further, the knockdown by *glmS* strategy is not absolute, it is also possible that the partial knockdown is not able to completely down-regulate the *Pf*LPL20 protein in the cell, and the remaining amount of *Pf*LPL20 is sufficient to carry out its required function for cell survival.

Extensive synthesis of membrane phospholipids is essential for parasite growth and segregation. Trophozoite and schizont infected erythrocytes show a six-fold increase in the phospholipid content in comparison to uninfected erythrocytes; most of this phospholipid content is phosphatidylcholine (PC), which is a major membrane phospholipid in *Plasmodium*. Under normal conditions, the parasite generated most of the required PC via CDP-Choline- dependent-Kennedy pathway using choline as a substrate [38-41]. Recent studies have shown that LPC imported from the serum is the main source of choline which converts into phosphocholine to get utilized for PC biosynthesis [9, 15], thus lysophospholipases play a key role in the membrane biosynthesis. The parasite can also

utilize triple methylation of the phosphoethanolamine (PE) to make phosphocholine which then enters in the same pathway to make PC (Figure 6). This involves the activity of phosphoethanolamine methyltransferase (PMT), which transfers a methyl group from S-adenosylmethionine (SAM) to PE. Further, under serum LPC depleted conditions, there is a shift of PC synthesis towards the PMT pathway using ethanolamine substrate [9]. It was also shown that under LPC depleted conditions the expression of *Pf*PMT (phosphoethanolamine-methyltransferase), *Pf*SAMS (S-adenosylmethionine synthetase), and *Pf*EK (ethanolamine kinase) are upregulated. The *Pf*LPL20 knockdown conditions may reduce catabolism of LPC and reduce the availability of choline for the Kennedy pathways, therefore transcript levels of different enzymes of PMT pathways were assessed. In *Pf*LPL20 knockdown conditions, there was a significant upregulation in the transcript level of *Pf*SAMS (SAM synthetase), whereas expression levels of *Pf*PMT and *Pf*EK were not altered. These results suggest that the transcript response under *Pf*LPL20 knockdown conditions was somewhat different as compared to LPC depleted conditions: upregulation of PMT transcript was reported in serum LPC depleted conditions [15]; in addition, there was upregulation of AP2-G transcript levels which resulted in induction of gametocytes. It is also shown that in field-isolates high plasma LPC has a negative influence on gametocyte production [42], it was suggested that the LPC depletion acts upstream of any event of sexual differentiation, but its exact role in induction of sexual commitment remains unclear.

In addition, quantitative evaluation of metabolites showed upregulation of phosphocholine as well as SAM levels in the *Pf*LPL20 knock-down conditions. This shows that upregulation of SAMS under *Pf*LPL20-iKD conditions resulted in increased conversion of L-methionine to SAM, resulting in the accumulation of SAM and thus its higher availability for triple methylation step by *Pf*PMT; consequently, the PMT pathway got upregulated to produce higher levels of phosphocholine. These results thus confirm that

under *Pf*LPL20 knockdown conditions, the alternate pathway gets upregulated to provide phosphocholine required for PC biosynthesis, which helps asexual stage parasites to survive and multiply. However, it is also possible that some other LPL in the parasite takes over the function to certain extents, to compensate the loss of *Pf*LPL20. We would also like to point out that knockdown of the *Pf*LPL20 protein in this study was not absolute, and therefore the remaining amount of *Pf*LPL20 may still carry out its functional role in the cell.

Overall, our results indicate *Pf*LPL20 plays a role in PC biosynthesis through catabolism of LPC acquired from host milieu to provide choline which gets phosphorylated to form the phosphocholine; under the *Pf*LPL20 depleted conditions, the parasite switches an alternate SDPM pathway for phosphocholine synthesis, which is utilized for PC biosynthesis. Thus, the parasite can compensate for the loss of one pathway of phosphocholine synthesis with another pathway, so that the parasite growth and segregation are being maintained. These results may suggest that *Pf*LPL20 levels regulate cooperation between two different pathways to generate phosphocholine required for PC synthesis. These data provide new information on membrane phospholipid biosynthetic pathways of the malaria parasite, which could be used to design future therapeutic approaches.

Acknowledgements

We are grateful to Philip J. Shaw for providing vector pGFP_glmS and useful suggestions; Siggi Sato for pSSPF2 vector. We thank Rotary blood bank, New Delhi for providing the RBCs. We thank Girish for his assistance in LC-MS analysis. PKS is supported by a research fellowship from the University Grant Commission, Govt. of India. MN was supported by a research fellowship from the Department of Biotechnology, Govt. of India. VT is supported by BioCARe Women Scientist Fellowship from the Department of Biotechnology, Govt. of India. The research work in AM's laboratory is supported by the Centre Of Excellence grant

(BT/COE/34/SP15138/2015) from the Department of Biotechnology, Govt. of India, and Indo-French Collaborative Research Program Grant (Project 6003-1) by the CEFIPRA.

References

1. World Health Organization., World Malaria Report 2020.
2. Weis, D.J., et al., Mapping the global prevalence, incidence, and mortality of *Plasmodium falciparum*, 2000–17: a spatial and temporal modelling study. Lancet, 2019 Jul 27;394(10195):322-331
3. Dechamps, S., et al., The Kennedy phospholipid biosynthesis pathways are refractory to genetic disruption in *Plasmodium berghei* and therefore appear essential in blood stages. Mol Biochem Parasitol, 2010. **173**(2): p. 69-80.
4. Botte, C.Y., et al., Atypical lipid composition in the purified relict plastid (apicoplast) of malaria parasites. Proc Natl Acad Sci U S A, 2013. **110**(18): p. 7506-11.
5. Asahi, H., et al., Investigating serum factors promoting erythrocytic growth of *Plasmodium falciparum*. Exp Parasitol, 2005. **109**(1): p. 7-15.
6. Haldar, K., et al., The accumulation and metabolism of a fluorescent ceramide derivative in *Plasmodium falciparum*-infected erythrocytes. Mol Biochem Parasitol, 1991. **49**(1): p. 143-56.
7. Greenspan, P., E.P. Mayer, and S.D. Fowler, Nile red: a selective fluorescent stain for intracellular lipid droplets. J Cell Biol, 1985. **100**(3): p. 965-73.
8. Gulati, S., et al., Profiling the Essential Nature of Lipid Metabolism in Asexual Blood and Gametocyte Stages of *Plasmodium falciparum*. Cell Host Microbe, 2015. **18**(3): p. 371-81.

9. Wein, S., et al., Contribution of the precursors and interplay of the pathways in the phospholipid metabolism of the malaria parasite. J Lipid Res, 2018. **59**(8): p. 1461-1471.

10. Bhanot, P., et al., A surface phospholipase is involved in the migration of *Plasmodium* sporozoites through cells. J Biol Chem, 2005. **280**(8): p. 6752-60.

11. Kilian, N., et al., Role of phospholipid synthesis in the development and differentiation of malaria parasites in the blood. J Biol Chem, 2018. **293**(45): p. 17308-17316.

12. Pessi, G., et al., In vivo evidence for the specificity of *Plasmodium falciparum* phosphoethanolamine methyltransferase and its coupling to the Kennedy pathway. J Biol Chem, 2005. **280**(13): p. 12461-6.

13. Pessi, G., G. Kociubinski, and C.B. Mamoun, A pathway for phosphatidylcholine biosynthesis in *Plasmodium falciparum* involving phosphoethanolamine methylation. Proc Natl Acad Sci U S A, 2004. **101**(16): p. 6206-11.

14. Bobenchik, A.M., et al., *Plasmodium falciparum* phosphoethanolamine methyltransferase is essential for malaria transmission. Proc Natl Acad Sci U S A, 2013. **110**(45): p. 18262-7.

15. Brancucci, N.M.B., et al., Lysophosphatidylcholine Regulates Sexual Stage Differentiation in the Human Malaria Parasite *Plasmodium falciparum*. Cell, 2017. **171**(7): p. 1532-1544 e15.

16. Hanada, K., et al., Neutral sphingomyelinase activity dependent on Mg2+ and anionic phospholipids in the intraerythrocytic malaria parasite *Plasmodium falciparum*. Biochem J, 2000. **346 Pt 3**: p. 671-7.

17. Hanada, K., et al., *Plasmodium falciparum* phospholipase C hydrolyzing sphingomyelin and lysocholinephospholipids is a possible target for malaria chemotherapy. J Exp Med, 2002. **195**(1): p. 23-34.

18. Raabe, A., et al., Genetic and transcriptional analysis of phosphoinositide-specific phospholipase C in *Plasmodium*. Exp Parasitol, 2011. **129**(1): p. 75-80.

19. Flammersfeld, A., et al., Phospholipases during membrane dynamics in malaria parasites. Int J Med Microbiol, 2018. **308**(1): p. 129-141.

20. Flammersfeld, A., et al., A patatin-like phospholipase functions during gametocyte induction in the malaria parasite *Plasmodium falciparum*. Cell Microbiol, 2020. **22**(3): p. e13146.

21. Singh, P., et al., Role of a patatin-like phospholipase in *Plasmodium falciparum* gametogenesis and malaria transmission. Proc Natl Acad Sci U S A, 2019. **116**(35): p. 17498-17508.

22. Istvan, E.S., et al., Esterase mutation is a mechanism of resistance to antimalarial compounds. Nat Commun, 2017. **8**: p. 14240.

23. Burda, P.C., et al., A *Plasmodium* phospholipase is involved in disruption of the liver stage parasitophorous vacuole membrane. PLoS Pathog, 2015. **11**(3): p. e1004760.

24. Schrag, J.D. and M. Cygler, Lipases and alpha/beta hydrolase fold. Methods Enzymol, 1997. **284**: p. 85-107.

25. Vial, H.J., M.J. Thuet, and J.R. Philippot, Phospholipid biosynthesis in synchronous *Plasmodium falciparum* cultures. J Protozool, 1982. **29**(2): p. 258-63.

26. Mitamura, T. and N.M. Palacpac, Lipid metabolism in *Plasmodium falciparum*-infected erythrocytes: possible new targets for malaria chemotherapy. Microbes Infect, 2003. **5**(6): p. 545-52.

27. Ben Mamoun, C., S.T. Prigge, and H. Vial, Targeting the Lipid Metabolic Pathways for the Treatment of Malaria. Drug Dev Res, 2010. **71**(1): p. 44-55.

28. Choubey, V., et al., Inhibition of *Plasmodium falciparum* choline kinase by hexadecyltrimethylammonium bromide: a possible antimalarial mechanism. Antimicrob Agents Chemother, 2007. **51**(2): p. 696-706.

29. Zidovetzki, R., et al., Inhibition of *Plasmodium falciparum* lysophospholipase by anti-malarial drugs and sulphydryl reagents. Parasitology, 1994. **108 (Pt 3)**: p. 249-55.

30. de Koning-Ward, T.F., P.R. Gilson, and B.S. Crabb, Advances in molecular genetic systems in malaria. Nat Rev Microbiol, 2015. **13**(6): p. 373-87.

31. Meissner, M., et al., Tetracycline analogue-regulated transgene expression in *Plasmodium falciparum* blood stages using Toxoplasma gondii transactivators. Proc Natl Acad Sci U S A, 2005. **102**(8): p. 2980-5.

32. Armstrong, C.M. and D.E. Goldberg, An FKBP destabilization domain modulates protein levels in *Plasmodium falciparum*. Nat Methods, 2007. **4**(12): p. 1007-9.

33. Jackson, K.E., et al., Food vacuole-associated lipid bodies and heterogeneous lipid environments in the malaria parasite, *Plasmodium falciparum*. Mol Microbiol, 2004. **54**(1): p. 109-22.

34. Palacpac, N.M., et al., Developmental-stage-specific triacylglycerol biosynthesis, degradation and trafficking as lipid bodies in *Plasmodium falciparum*-infected erythrocytes. J Cell Sci, 2004. **117**(Pt 8): p. 1469-80.

35. Zhang, M., et al., Uncovering the essential genes of the human malaria parasite *Plasmodium falciparum* by saturation mutagenesis. Science, 2018. **360**(6388).

36. Biagini, G.A., et al., Characterization of the choline carrier of *Plasmodium falciparum*: a route for the selective delivery of novel antimalarial drugs. Blood, 2004. **104**(10): p. 3372-7.

37. Ancelin, M.L., et al., Increased permeability to choline in simian erythrocytes after *Plasmodium* knowlesi infection. Biochem J, 1991. **273 (Pt 3)**: p. 701-9.

38. Ancelin, M.L. and H.J. Vial, Regulation of phosphatidylcholine biosynthesis in *Plasmodium*-infected erythrocytes. Biochim Biophys Acta, 1989. **1001**(1): p. 82-9.

39. Carman, G.M. and S.A. Henry, Phospholipid biosynthesis in yeast. Annu Rev Biochem, 1989. **58**: p. 635-69.

40. Kent, C., Eukaryotic phospholipid biosynthesis. Annu Rev Biochem, 1995. **64**: p. 315-43.

41. Lykidis, A. and S. Jackowski, Regulation of mammalian cell membrane biosynthesis. Prog Nucleic Acid Res Mol Biol, 2001. **65**: p. 361-93.

42. Usui, M., et al., *Plasmodium falciparum* sexual differentiation in malaria patients is associated with host factors and GDV1-dependent genes. Nat Commun, 2019. **10**(1): p. 2140.

43. Crabb, B.S., et al., Transfection of the human malaria parasite *Plasmodium falciparum*. Methods Mol Biol, 2004. **270**: p. 263-76.

44. Prommana, P., et al., Inducible knockdown of *Plasmodium* gene expression using the glmS ribozyme. PLoS One, 2013. **8**(8): p. e73783.

45. Mimmi, M.C., et al., Absolute quantification of choline-related biomarkers in breast cancer biopsies by liquid chromatography electrospray ionization mass spectrometry. Anal Cell Pathol (Amst), 2013. **36**(3-4): p. 71-83.

Figure Legends:

Figure 1: Production of recombinant *Pf*LPL20 and enzyme kinetics analysis: (A) Domain organization of *Pf*LPL20 showing transmembrane domain at N- terminus and two hydrolase-like domains, location of the active site residues are shown. (B) SDS-PAGE gel showing purified recombinant *Pf*LPL20 protein used for activity assay. (C) Graphical representation of LPL activity of *Pf*LPL20 in presence of the varying amount of protein (10, 15, and 20 μg); relative fluorescence unit (RFU) generated in each assay in time depended manner are shown. (D) Line graph of Michaelis-Menten fit for *Pf*LPL20 activity in presence of the 20μg (85pmoles) of recombinant protein. The *K*m value of *Pf*LPL20 was found to 33.41 μM.

Figure 2: Generation of transgenic parasite line expressing *Pf*LPL20-GFP fusion protein and sub-cellular localisation of *Pf*LPL20: (A) Western blot analysis of lysate of transgenic parasites using anti-GFP antibody shows a band at ~70 kDa, which was not detected in the wild-type 3D7 parasite lysate; a parallel blot probed with anti-BiP antibodies to show equal loading. (B) Confocal microscopy images of the transgenic parasites at ring, trophozoite, and schizont stages expressing fusion protein. *Pf*LPL20-GFP fusion protein was present in the vesicular structures near parasite boundary, in the cytosol, and as a large multi-vesicle like structure near the food-vacuole. (C) Co-staining of transgenic parasites with neutral lipid marker (Nile red) shows that the *Pf*LPL20 (green) associates with neutral lipid storage body near the food-vacuole. The nucleus was stained in blue with DAPI.

Figure 3: Generation of transgenic parasite line with GFP-*glmS* tag in the *pfLPL20* gene locus for transient knock-down: (A) Schematic representation of GFP-*glm*S reverse genetic approach showing the integration of *Pf*LPL20-GFP-glmS plasmid at the C-terminus

of the endogenous *pflpl20* gene locus. (B) PCR-based analyses to confirm integration of plasmid in the target gene locus using total DNAs of the transgenic parasite culture (purified clonal parasite population) and wild type 3D7 parasite lines; locations of primers used and length of respective amplicons are marked in the schematic. Lane 1 and 4 (primers 2200_F and 1234A) showing amplification only in the integrants; lane 2 and 4 (primers 1224A and 1234A) show amplification in integrants or episome parasites; lane 3 and 6 (primers number 1224A and 1225A) show amplification in both integrants and the wild-type line. (C) Western blot analysis of lysate of transgenic and wild-type parasites using an anti-GFP antibody. The fusion protein band (~70kDa) was detected in the transgenic parasites only (lane 2) and not in the wild-type parasite (lane 1). Blot ran in parallel with an equal amount of the same sample, probed with anti-BiP, was used as a loading control. (D) Western blot analysis of lysate of transgenic at different developmental stages using anti-GFP antibody: lane 1, ring stage; lane 2, trophozoite stages; and lane 3, schizont stages. (E) Fluorescent microscopic images of transgenic parasites. Fusion protein signal was observed in vesicular structures in transgenic parasites. The parasite nuclei were stained with DAPI and parasites were visualized by a confocal laser scanning microscope. (F) *Pf*LPL20 associate with a neutral lipid storage body near the food vacuole. Fluorescence images of trophozoites stage transgenic parasites expressing *Pf*LPL20-GFP stained with Nile Red, a neutral lipid staining dye. The large GFP labelled structure close to the food vacuole (having dark hemozoin) showed staining with Nile Red. The parasite nuclei were stained with DAPI (blue) and parasites were visualized by a confocal laser scanning microscope.

Figure 4: Inducible knock-down showing dispensability of *Pf*LPL20 in asexual blood stages of the parasite: (A) Western blot analysis using anti-GFP antibody showing a reduction in the *Pf*LPL20-GFP fusion protein levels in transgenic parasites grown in

presence of 2.5 mM glucosamine (+GlcN) as compared to control (-GlcN); a blot ran in parallel with an equal amount of the same sample was probed with anti-Bip antibodies as a loading control. (B) Graph showing quantitative levels of *Pf*LPL20-GFP fusion protein in the western blot analysis as determined by densitometric analysis. (C) Graph showing *Pf*LPL20-GFP-*glmS* parasite growth in presence of 2.5 mM glucosamine (+GlcN) as compared to control (-GlcN). Tightly synchronized ring-stage parasite culture of transgenic parasites grown with or without glucosamine (Control and *Pf*LPL20-iKO, respectively), and their growth was monitored as the formation of new rings estimated 48 and 96h. The *p* values were calculated by Student's *t*-test: *ns* for $p > 0.1$. The reduction in parasite growth was found to be statistically non-significant (*p* value >0.8). (D) Morphological analysis of the parasites from control and *Pf*LPL20 knock-down sets at the ring, trophozoite, and schizont stage. *Pf*LPL20-iKD parasite showed a slight delay in development into schizont as compared to the control set, however, all the parasites developed into schizonts formed segregated merozoites, and developed new ring-stage parasites.

Figure 5: Effect of *Pf*LPL20 knock-down renders parasite to upregulate alternate SDPM pathway for phosphocholine synthesis: (A) Graphical representation of relative transcript levels of different genes of the SDPM pathway in *Pf*LPL20-iKD parasites as compared to control set. Expression of *Pf*SAMS was altered significantly while there was no change in the expression of *Pf*PMT and *Pf*EK. (B-D) Bar graph showing relative levels of choline (B), phosphocholine (C), and SAM (D) in *Pf*LPL20-iKD parasites in comparison to the control set. PMT: Phosphoethanolamine-N-methyltransferase, SAMS: S-adenosylmethionine synthetase, EK: ethanolamine kinase. Each experiment was carried out in triplicate. The *p* values were calculated by Student's *t*-test: * $p < 0.01$, ** $p < 0.005$ and *ns* for $p > 0.1$. Error bars indicate standard deviation of the mean for each set of data.

Figure 6: Schematic diagrams showing pathways for biosynthesis of major phospholipids (PC, PE, PS) in *Plasmodium* and effect of *Pf*LPL20-iKD on these pathways: The parasite scavenges both choline and LPC from host milieu; however, the choline generated by catabolization of LPC, gets phosphorylated into phosphocholine, which enters in the Kennedy pathway for PC synthesis. Ethanolamine and Serine taken up from host milieu are phosphorylated into P-Etn and utilized for the synthesis of PE and PS. Methionine and Serine are also generated from the catabolism of hemoglobin in the food-vacuole. In *Pf*LPL20-iKD conditions, the choline generated from LPC is reduced, the SAMS gets upregulated which leads to higher production of SAM which is utilized by PMT to generate phosphocholine to compensate for the loss of choline/phosphocholine. LPC, Lysophosphatidylcholine; LPL20 ; lysophospholipase 20; PL, Phospholipase, Cho, choline; CK, choline kinase; CCT, CTP:phosphocholine cytidylyltransferase; CDP-Cho, CDP-choline; CEPT, choline/ethanolamine-phosphotransferase; PC, Phosphatidylcholine; Met, Methionine; SAMS, SAM synthetase; SAM, S-adenosylmethionine; PMT, Phosphoethanolaminemethyltransferase; Etn, Etanolamine; EK, ethanolamine kinase; P-Etn, phosphoethanolamine; ECT, CTP:phosphoethanolamine cytidylyltransferase; CDP-Etn, CDPethanolamine; CEPT, choline/ethanolaminephosphotransferase; PE, Phosphoethanolamine; Ser, Serine; CSPT, CDP-diacylglycerol-serine-O-phosphatidyltransferase; PSS2, phosphatidylserine synthase by base exchange type 2; PSD, phosphatidylserine decarboxylase, FV, food vacuole; Hb, hemoglobin.

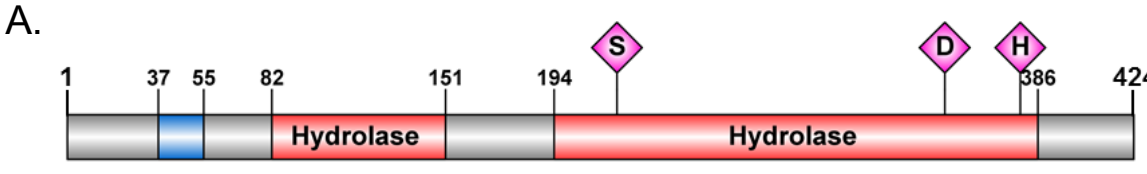
A.
1
37
55
82
151
194
S
D
H
386
424
Hydrolase
Hydrolase

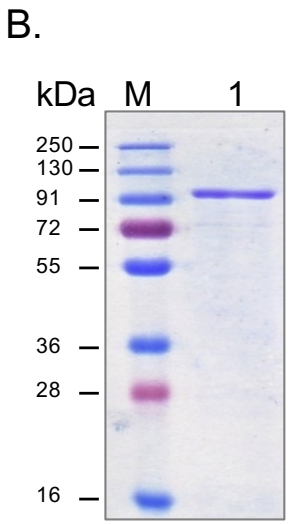
B.
kDa
M
1
250
130
91
72
55
36
28
16

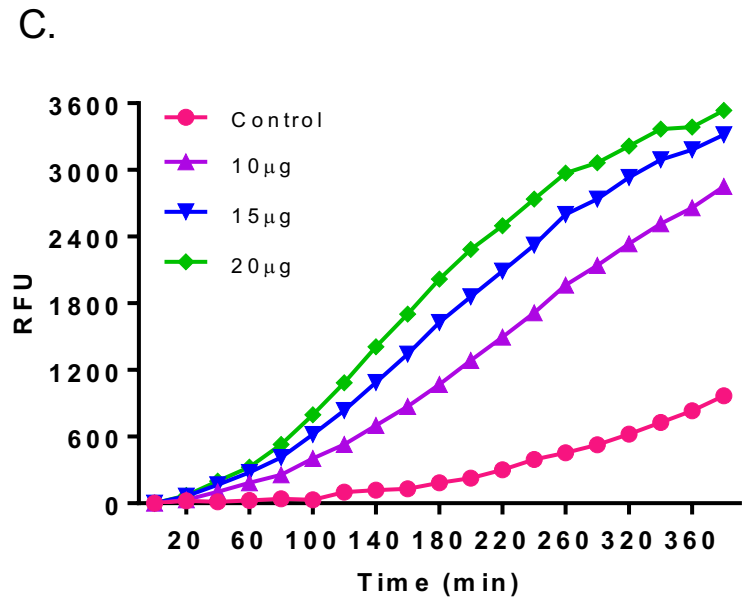
C.
3600
3000
2400
1800
1200
600
0
RFU
Control
10μg
15μg
20μg
20
60
100
140
180
220
260
320
360
Time (min)

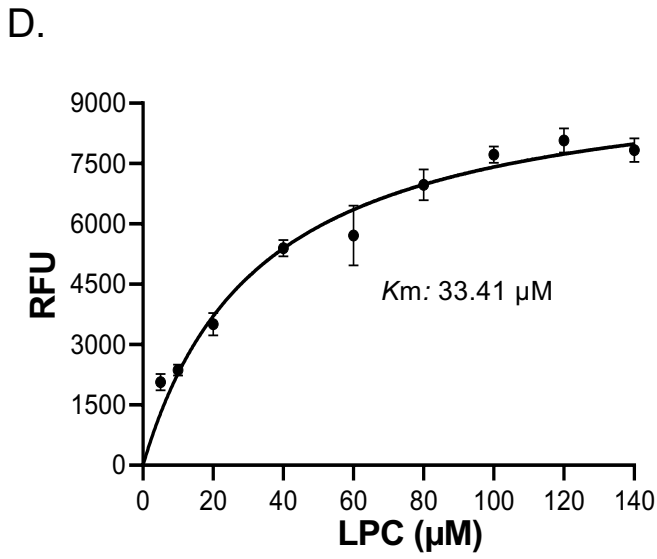
D.
9000
7500
6000
4500
3000
1500
0
RFU
Km: 33.41 μM
0
20
40
60
80
100
120
140
LPC (μM)

Figure 1

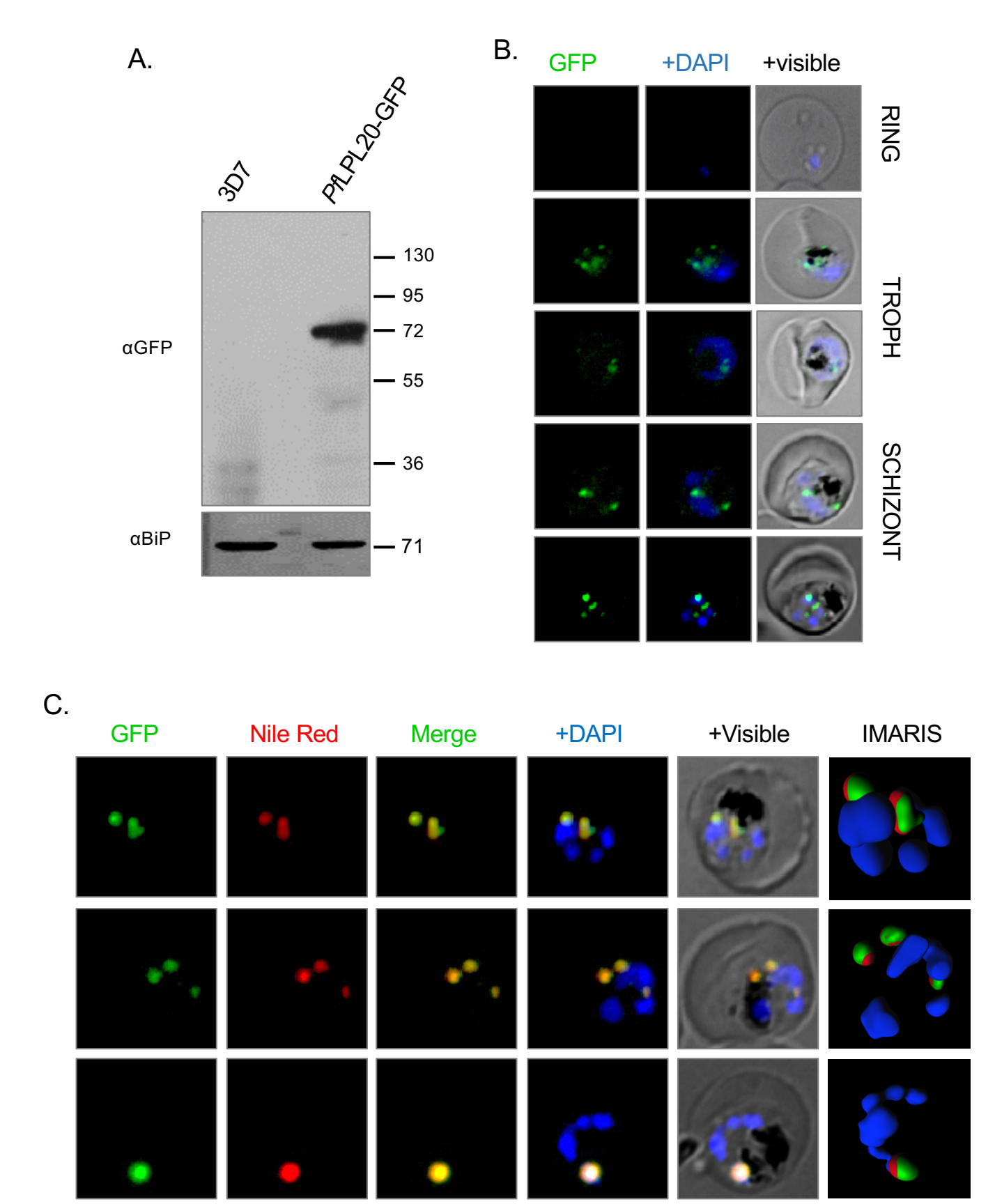
A.
3D7
PfLPL20-GFP
αGFP
αBiP
130
95
72
55
36
71
B.
GFP
+DAPI
+visible
RING
TROPH
SCHIZONT
C.
GFP
Nile Red
Merge
+DAPI
+Visible
IMARIS

Figure 2

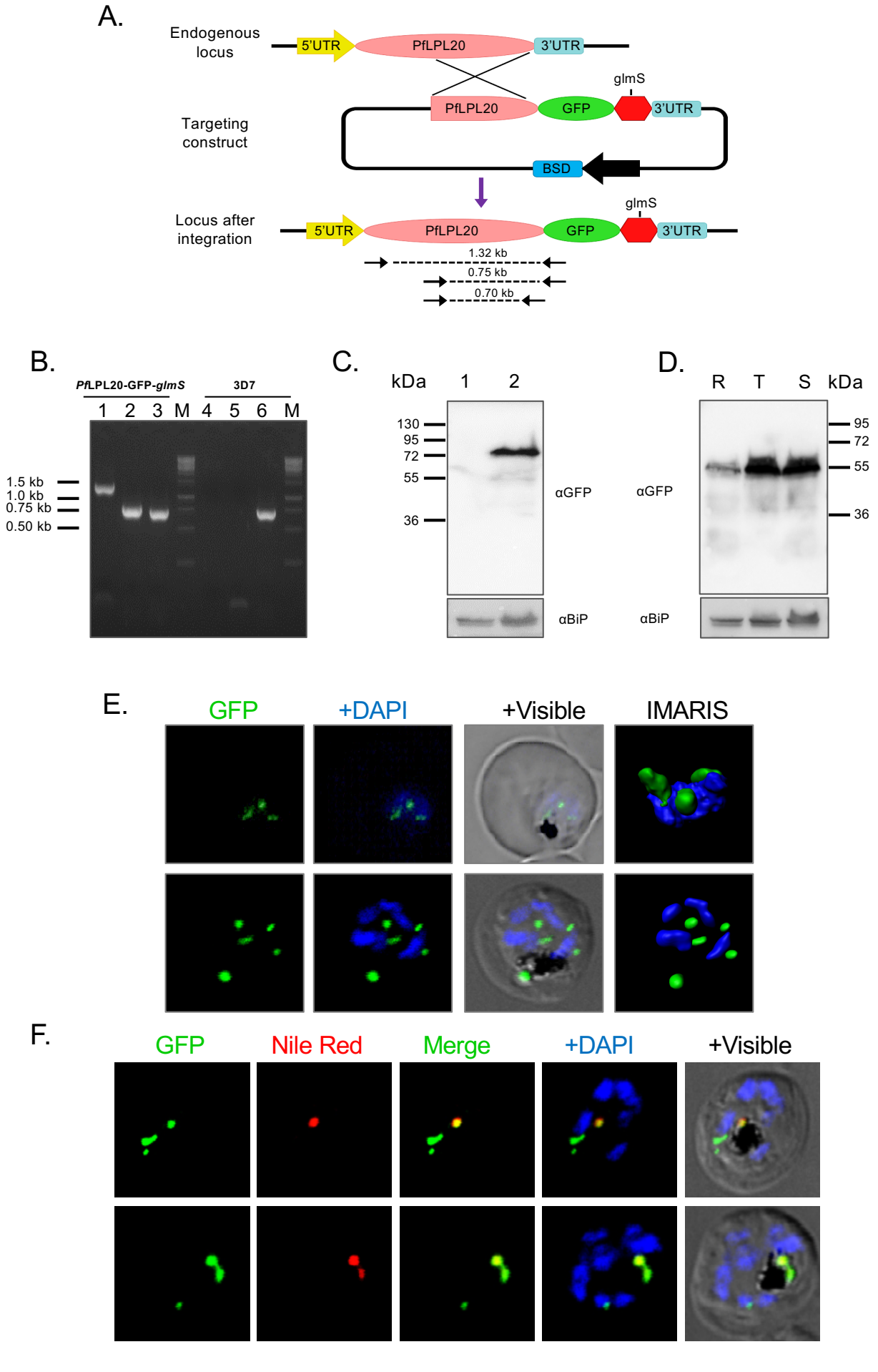

Figure 3

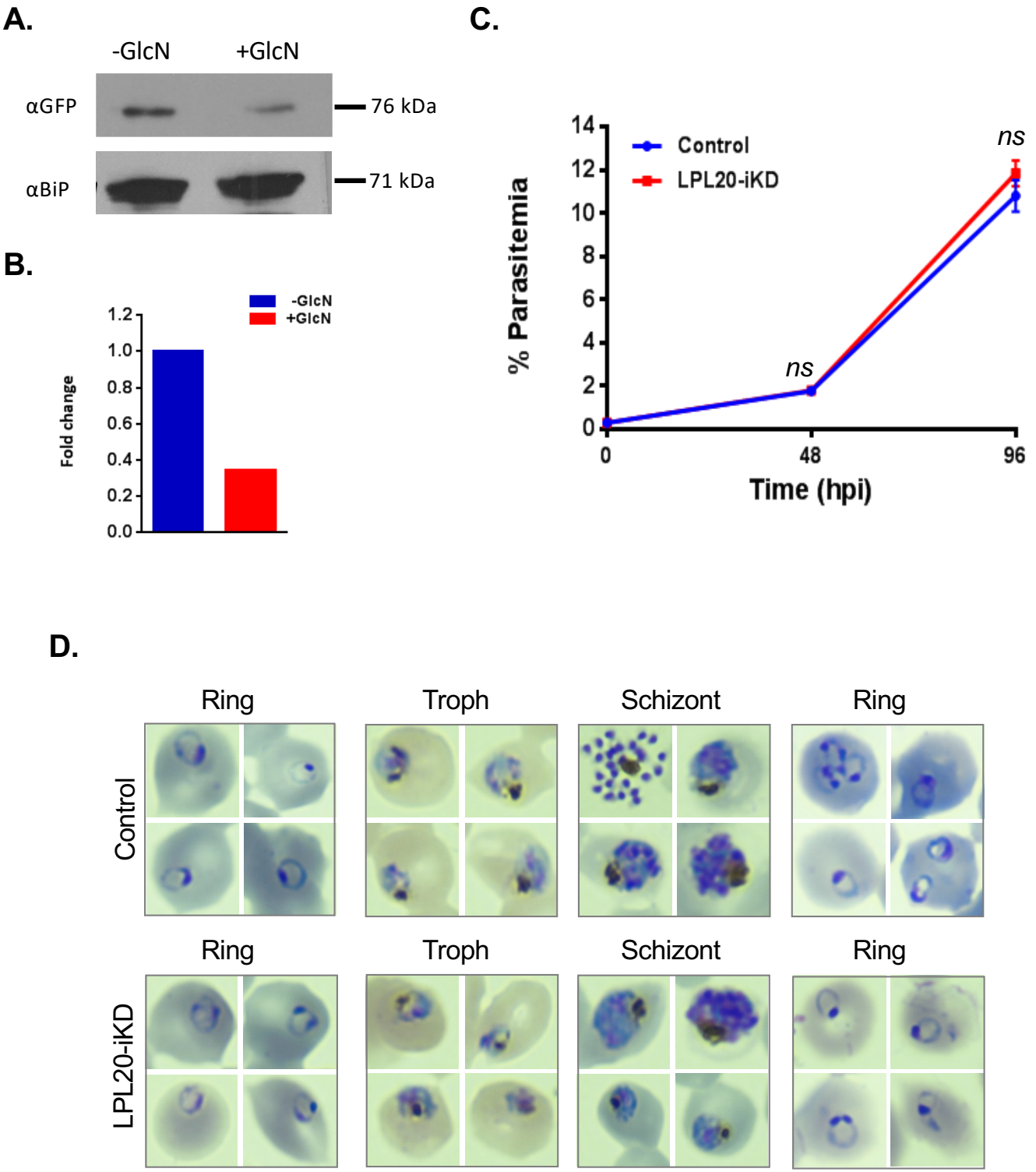
A.
-GlcN
+GlcN
αGFP
76 kDa
αBiP
71 kDa
B.
-GlcN
+GlcN
Fold change
1.2
1.0
0.8
0.6
0.4
0.2
0.0
C.
Control
LPL20-iKD
% Parasitemia
14
12
10
8
6
4
2
0
ns
ns
0
48
96
Time (hpi)
D.
Ring
Troph
Schizont
Ring
Control
Ring
Troph
Schizont
Ring
LPL20-iKD

Figure 4

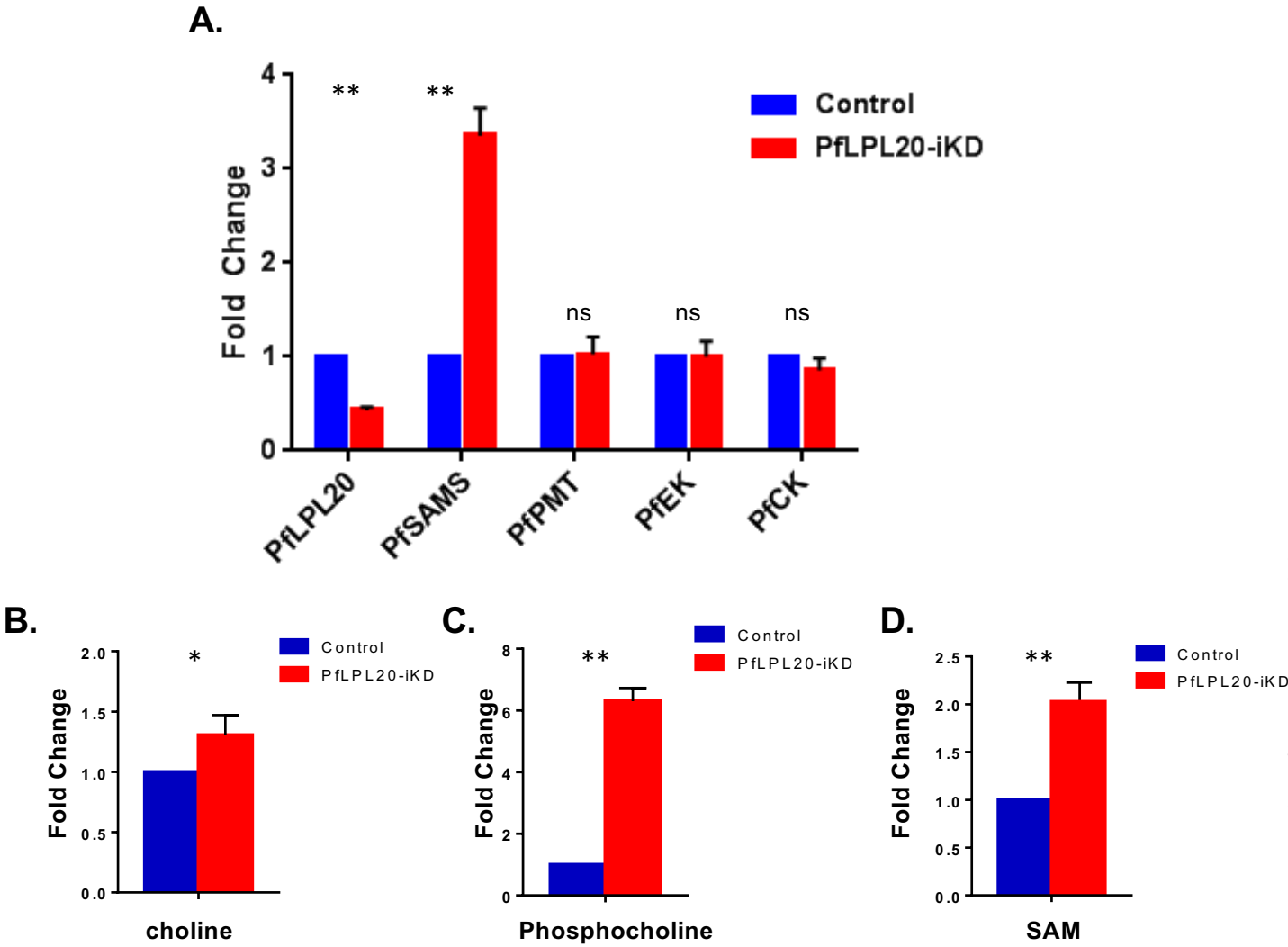

Figure 5